NuSTAR on-ground calibration II: Effective area

Nicolai F. Brejnholt[a], Finn E. Christensen[a], Niels J. Westergaard[a], Charles J. Hailey[b], Jason E. Koglin[c], William W. Craig[d]

[a]DTU Space, Technical University of Denmark, Copenhagen, Denmark
[b]Columbia University Astrophysics Laboratory, New York City, USA
[c]SLAC National Accelerator Laboratory, Menlo Park, USA
[d]Lawrence Livermore National Laboratory, Livermore, USA

ABSTRACT

The Nuclear Spectroscopic Telescope ARray (`NuSTAR`) was launched in June 2012 carrying the first focusing hard X-ray ($5-80$ keV) optics to orbit. The multilayer coating was carried out at the Technical University of Denmark (`DTU Space`). In this article we introduce the `NuSTAR` multilayer reference database and its implementation in the `NuSTAR` optic response model. The database and its implementation is validated using on-ground effective area calibration data and used to estimate in-orbit performance.

Keywords: X-ray calibration, NuSTAR, hard X-rays, multilayers, optic response

1. INTRODUCTION

The Nuclear Spectroscopic Telescope Array (`NuSTAR`)[1] is a `NASA` Small Explorer mission that launched on June 13, 2012 and achieved first light on June 28, 2012. The on-ground calibration of the two multilayer coated flight optics was carried out at the Rainwater Memorial Calibration Facility for X-ray optics (`RaMCaF`)[2,3] at Nevis Laboratories in New York. The multilayer coating was laid down at the Technical University of Denmark (`DTU Space`)[4].

`NuSTAR` is the first focusing hard X-ray ($5-80$ keV) telescope in orbit. The optics have undergone extensive on-ground calibration to address the unique challenges associated with the low graze angles, multilayer coatings and broad bandpass. In addition to the on-ground calibration, a suite of supporting measurements has been carried out, specifically to determine the in-situ figure error[5], specular and non-specular reflectivity, and coating non-uniformity of the mounted substrates. On their own, these data sets act to qualify critical aspects of the optic build, while together, they allow for the optic response model (`ORM`) to be constructed, as illustrated in Figure 1.

In the present article it is described how the `ORM` construction is facilitated by setting up the multilayer reference database (`MRD`). The `MRD` tracks run-to-run variations in coating chamber parameters and coating non-uniformity based on specular reflectivity measurements carried out at `RaMCaF` and `DTU Space`. As such, the `MRD` replaces the multilayer design presented by Christensen et al.[4] and summarized in Table 1.

The article goes on to describe the utilization of the `MRD` implementation in a ray tracing code[8] to estimate the effective area (A_{eff}) of each of the flight modules. The result of the ray trace effectively constitutes the `ORM` when coupled with the `MRD`. The `ORM` is validated using on-ground calibration data and in-orbit performance is estimated. Additional qualification of the `ORM` will be carried out using in-orbit calibration data, when available.

The image quality of `NuSTAR`, as predicted by the `ORM`, is described elsewhere in these proceedings[6]. For a more in-depth description of the measurement campaigns summarized in this paper refer to Brejnholt et al.[3], Brejnholt[7] and Koglin et al.[9].

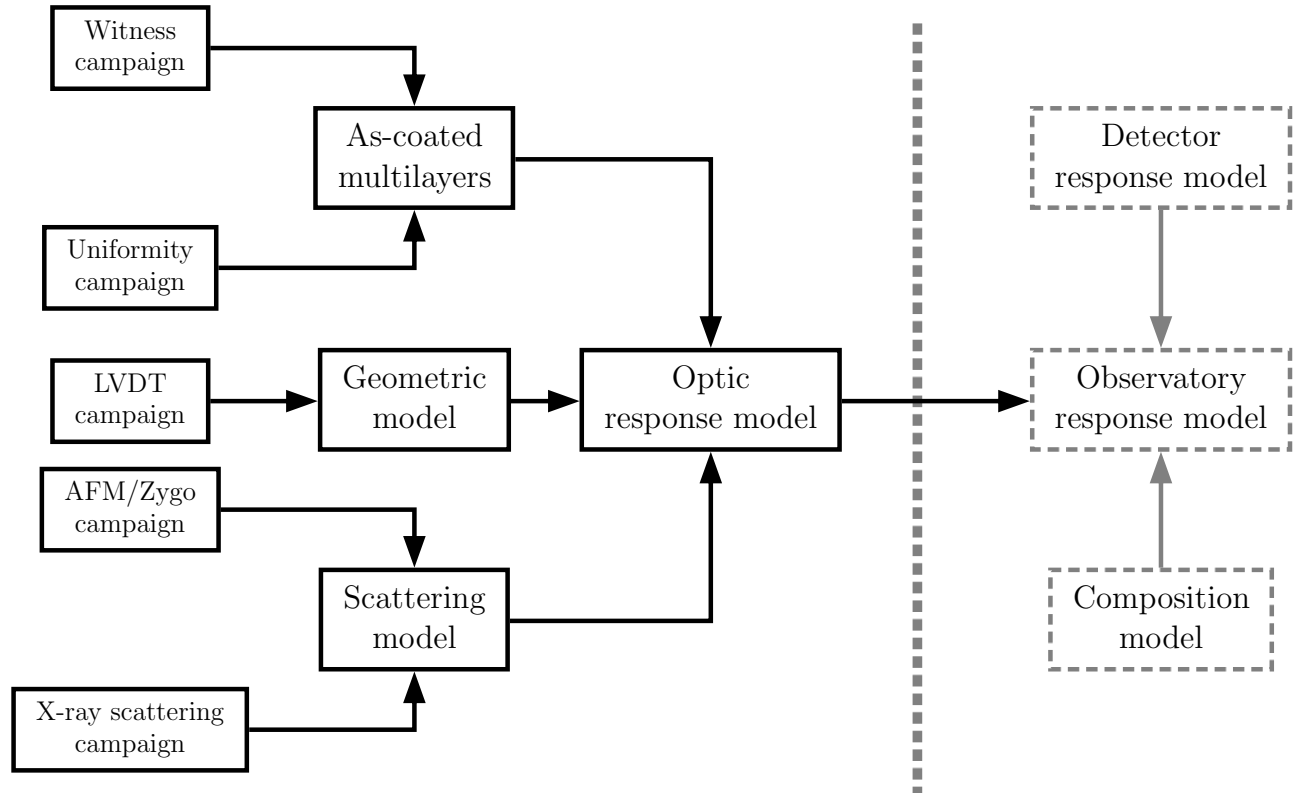Further author information: N.F.B.: E-mail: nicolai@space.dtu.dk, Telephone: +45 45 25 97 91

Figure 1. Overview of the main components of the ORM. The as-coated multilayers combine with a master table of substrates mounted in the optics to create the multilayer reference database described in Section 2. The components for the geometric and scattering models are described elsewhere in these proceedings[6]. Right of the dashed line indicates the final stage of integrating the ORM into the full NuSTAR observatory response model. Figure taken from Brejnholt[7].

Table 1. Overview of the intended multilayer recipes. Note that Γ_{top} applies only to the top bilayer (i.e. $N = 1$, which has the thickness d_{max}). The thicker heavy material improves total external reflectivity efficiency significantly below the critical energy. Additional details regarding the recipes are available from Christensen et al.[4].

Recipe	Materials	Layer range	α_i range [°]	d_{min} [Å]	d_{max} [Å]	N	c	Γ_{top}	Γ	σ[Å]
0	Pt/SiC	1	0.077	31.7	128.1	150	0.245	0.70	0.45	4.5
1	Pt/C	2-12	0.078-0.087	29	133.7	145	0.245	0.70	0.45	4.5
2	Pt/C	13-24	0.088-0.097	29	131.6	145	0.228	0.70	0.45	4.5
3	Pt/C	25-36	0.098-0.111	29	129.6	145	0.234	0.70	0.45	4.5
4	Pt/C	37-49	0.112-0.127	29	121.8	145	0.214	0.70	0.45	4.5
5	Pt/C	50-62	0.128-0.143	29	109.5	145	0.225	0.70	0.45	4.5
6	Pt/C	63-76	0.145-0.163	29	107.5	145	0.225	0.70	0.45	4.5
7	Pt/C	77-89	0.165-0.184	29	102.8	145	0.212	0.70	0.45	4.5
8	W/Si	90-104	0.186-0.210	25	95.2	291	0.238	0.80	0.38	4.3
9	W/Si	105-118	0.212-0.237	25	83.9	291	0.220	0.80	0.38	4.3
10	W/Si	119-133	0.242-0.270	25	74.5	291	0.190	0.80	0.38	4.3

2. MULTILAYER REFERENCE DATABASE

To track the run-to-run variations of the multilayers, each coating run included a flat Silicon (`Si`) wafer witness sample. Specular reflectivity data was acquired from the majority of the witness samples at `RaMCaF`. The reflectivity data was in turn used to estimate the as-coated multilayer, i.e. to determine d-spacing and heavy-to-light material ratio (Γ) progression through the stack, as well as micro-roughness (σ). Table 2 contains a summary of the witness campaign results. The as-coated multilayers are generally thinner than intended as a result of a tight production schedule preventing regular recalibration of the deposition rate. The distribution of the deviations from the intended coating are illustrated in Figure 2, where the relative d_{max} values are plotted versus relative d_{min}.

Table 2. Summary of witness campaign results. Data was acquired off thin `Si` wafer samples included in each flight coating run. Seventeen witness samples were not measured. $d_{min,wit}$, $d_{max,wit}$, Γ_{wit} and $\Gamma_{top,wit}$ describe the mean relative value compared to the design parameters (refer to Table 1), while σ_{wit} describes the mean witness sample micro-roughness, irrespective of the material combination. Note that the micro-roughness is on average 15% higher on slumped glass (refer to Table 3 and Christensen et al. [4]) compared to the `Si` wafer value given here.

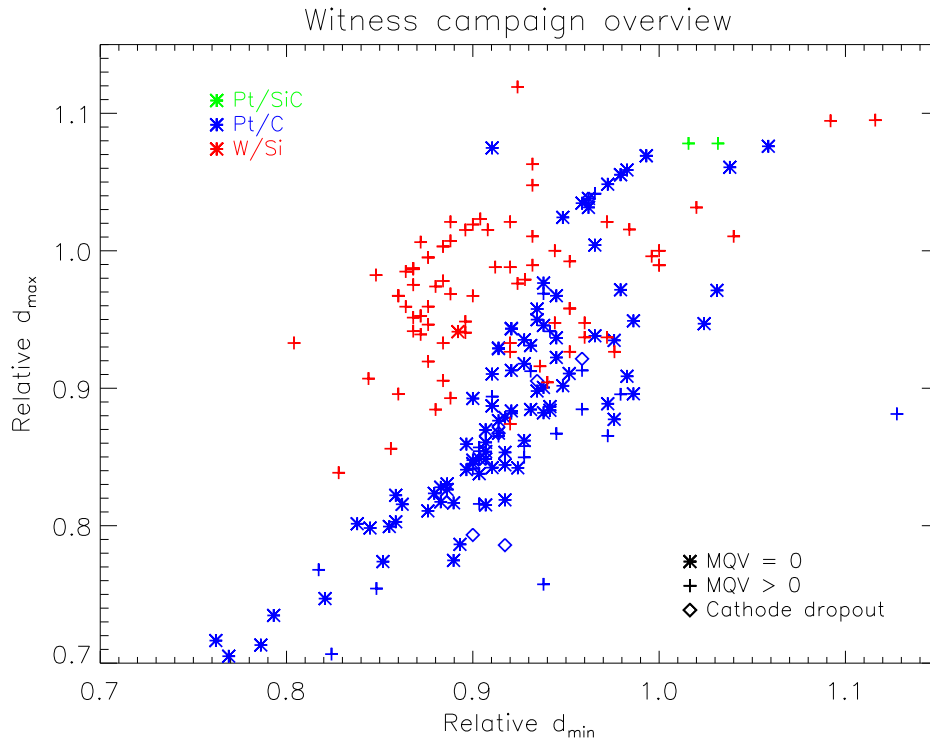| #Samples	239 (17)
Bandpass	10-100 keV
$d_{min,wit}$	91%
$d_{max,wit}$	92%
Γ_{wit}	99%
$\Gamma_{top,wit}$	100%
σ_{wit}	4.2 Å

Figure 2. Relative d_{max} plotted versus relative d_{min}. Infrequent recalibration of the deposition rate caused a bias towards thinner multilayers being laid down. Had this not been the case, one would expect the values to be packed closer around $d_{max} = 1.0$ and $d_{min} = 1.0$. Runs suspected of having cathode dropouts are marked separately, as they induce significant uncertainty in the as-coated multilayer model. For more information about the cathode dropouts, refer to Brejnholt [7].
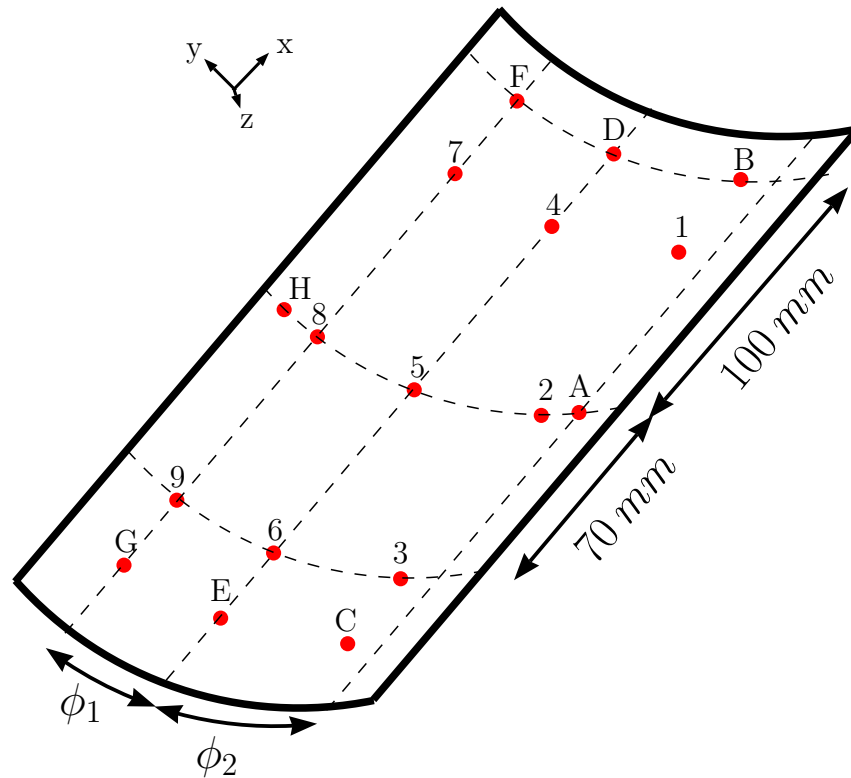
Figure 3. Overview of uniformity measurement points on spare flight substrates. For substrates with a full span of $30°$, $\phi_1 \approx 9.5°$ and $\phi_2 \approx 12.5°$ while for $60°$ segments $\phi_1 \approx 19°$ and $\phi_2 \approx 25°$. Refer to Brejnholt [7] for additional details on the measurements.

Table 3. Summary of uniformity campaign results. d_{uni}, Γ_{uni} and σ_{uni} describe the mean deviation from a uniform coating laid down on a substrate, as compared to a witness sample, while $d_{low,uni}$ and $d_{high,uni}$ indicate the extremes of the deviations. σ_{uni} indicates that micro-roughness is on average 15% higher on slumped glass compared to Si wafers (refer to Table 2 and Christensen et al. [4]).

#Substrates	25
#Points	421
d_{uni}	92%
$d_{low,uni}$	63%
$d_{high,uni}$	117%
Γ_{uni}	97%
σ_{uni}	115%

A map of the deposited coating's uniformity as a function of chamber location is required to relate the as-coated multilayer of a witness sample to the one laid down on the curved flight substrates. The uniformity map was constructed by conducting a series of constant d-spacing coating runs. The runs produced witness samples and curved substrates from all mounting configurations used during the flight coating campaign. The d-spacing, Γ and micro-roughness were determined in up to seventeen points distributed over the curved substrate surface and related to the witness sample parameters. The relative change in the parameters make up the uniformity map. The location of the seventeen points is shown in Figure 3. Table 3 contains a summary of the uniformity campaign results.

For any given substrate a master look-up table exists to identify its mounting location in the optic, as well as its associated witness sample and chamber location during coating. Combining the master table with the as-coated multilayer described above yields the MRD.

3. MT_RAYOR

The variations in the as-coated multilayer over the surface of individual flight substrates, contribute to the necessity of carrying out ray tracing to accurately evaluate A_{eff}. Ray tracing is carried out in the Yorick-based tool called MT_RAYOR[8]. MT_RAYOR implements a detailed representation of a NuSTAR optic and the RaMCaF facility, as well as in-situ measurements of all mounted substrate's figure error. For additional details on MT_RAYOR and the NuSTAR implementation, refer to Westergaard et al.[6] (these proceedings) and Westergaard[8].

4. ON-GROUND CALIBRATION

No end-to-end on-ground calibration of the observatory was carried out. The on-ground calibration of the two stand-alone optics was carried out in March 2011. More than fifty thousand unique spectra are available from the eighteen-day long campaign, roughly ten thousand of which constitutes the core calibration data set. The large volume of measurements cover both on- and off-axis response with finite source distance as well as subgroup measurements seeking to imitate an infinite source distance. The pseudo-infinite illumination was enabled by selecting a small section of the optic (a subgroup) and aligning the optic axis to that of the divergent beam at the relevant radius. The strength of the on-ground calibration data set, compared to in-orbit data, derives from these subgroup measurements, where only a small fraction of the optic is investigated, effectively improving the resolution of the ORM validation. Detailed accounts of the calibration approach and hardware are available from Brejnholt et al.[2], Brejnholt et al.[3] and Koglin et al.[9].

5. ON-GROUND CALIBRATION DATA

To most readily evaluate the quality of the ORM, single reflection data from the on-ground calibration is used. The geometry used for acquiring this data set is sketched in Figure 4. As only the upper shells of the Wolter-I optic contribute in this setup, the data consists of summed contributions from as few as six mounted substrates, rather than summed and convolved contributions from twice that amount of mounted substrates in the double reflection case discussed below. In general these comparisons imply that the ORM describes the optics well. An example of this is shown in Figure 5.

One major caveat with the single reflection data, however, is that it can at most sample half of the mounted substrate area. Outside of in-orbit data, the double reflection subgroup measurements are the only way to sample the entire surface area of the mounted substrates. The geometry used for acquiring this data set is sketched in Figure 6. At the time of writing only a small subset of the double reflection data has been investigated. Early indications imply that the ORM provides a good prediction for the on-ground calibration data. A preliminary comparison between model and data is shown in Figure 7.
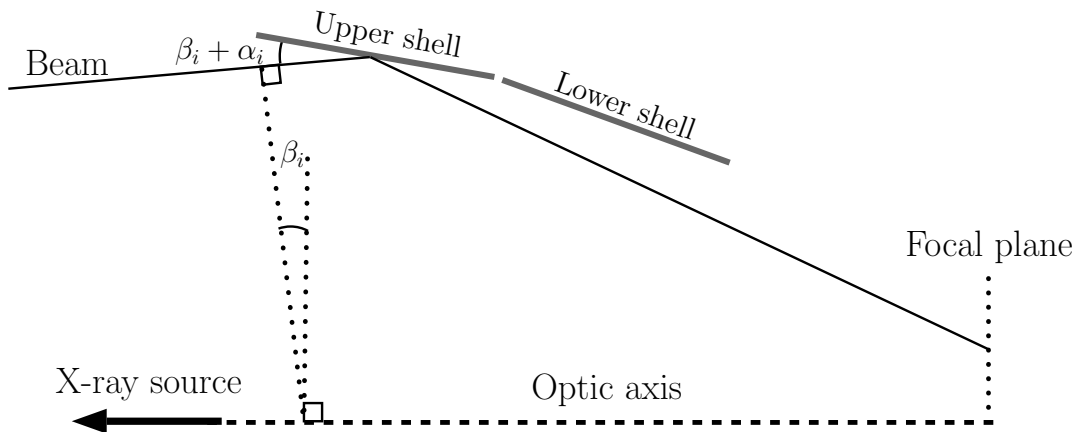

Figure 4. Single reflection geometry. α_i is the grazing incidence angle (refer to Table 1) for layer i, while β_i corresponds to the beam angle for said layer, i.e. the beam divergence at a given radius and finite source distance (163.1 m at RaMCaF). A minimum of six upper shells contribute to the single reflection data acquired.
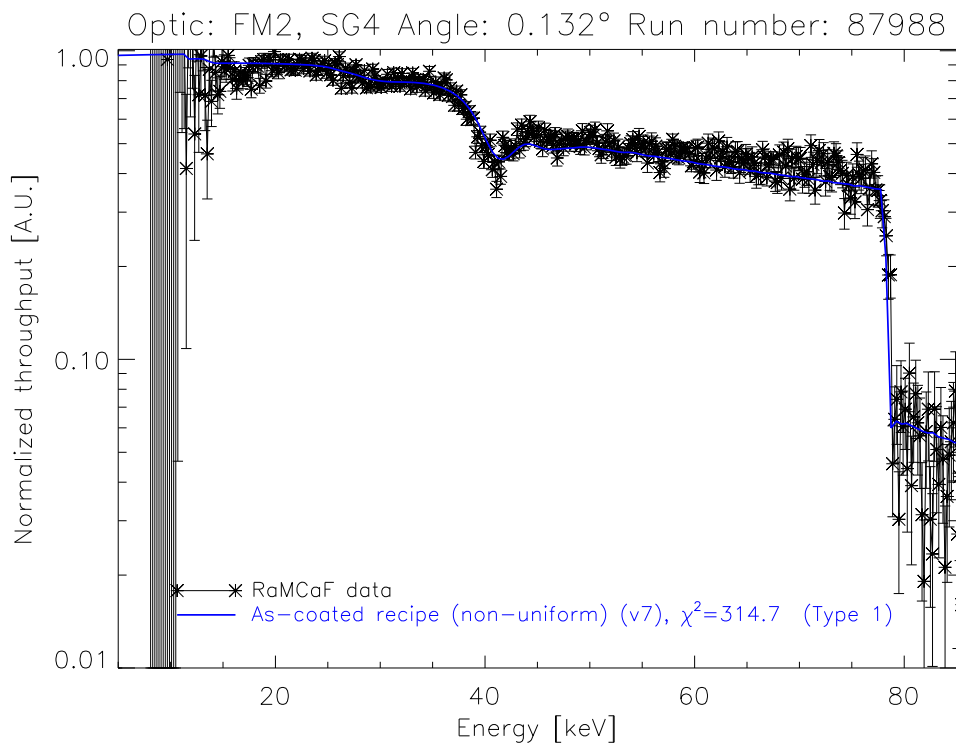
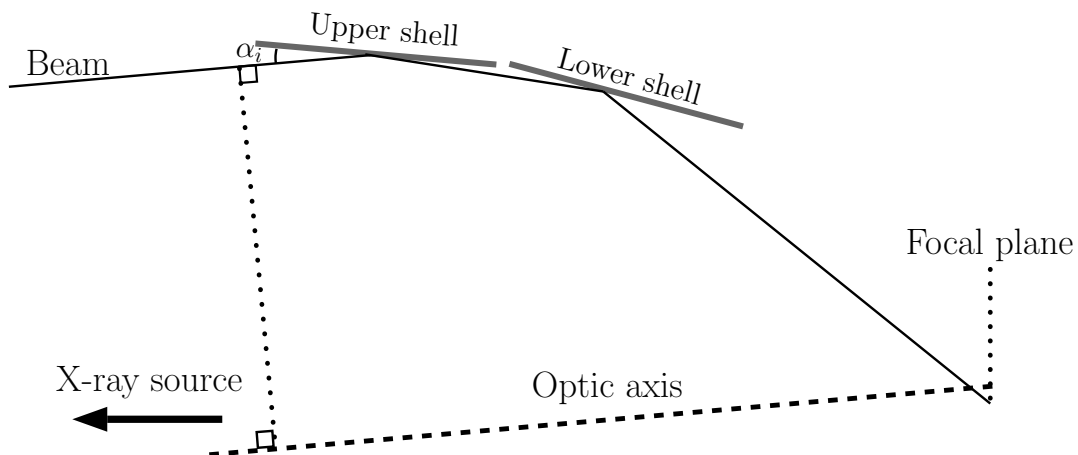Figure 5. `ORM` prediction of reflectivity for a single reflection subgroup measurement.

Figure 6. Double reflection geometry. Contrary to Figure 4 the optic axis is aligned to the beam during double reflection measurements, to imitate a parallel beam. A minimum of twelve upper and lower shells contribute to the double reflection data acquired.
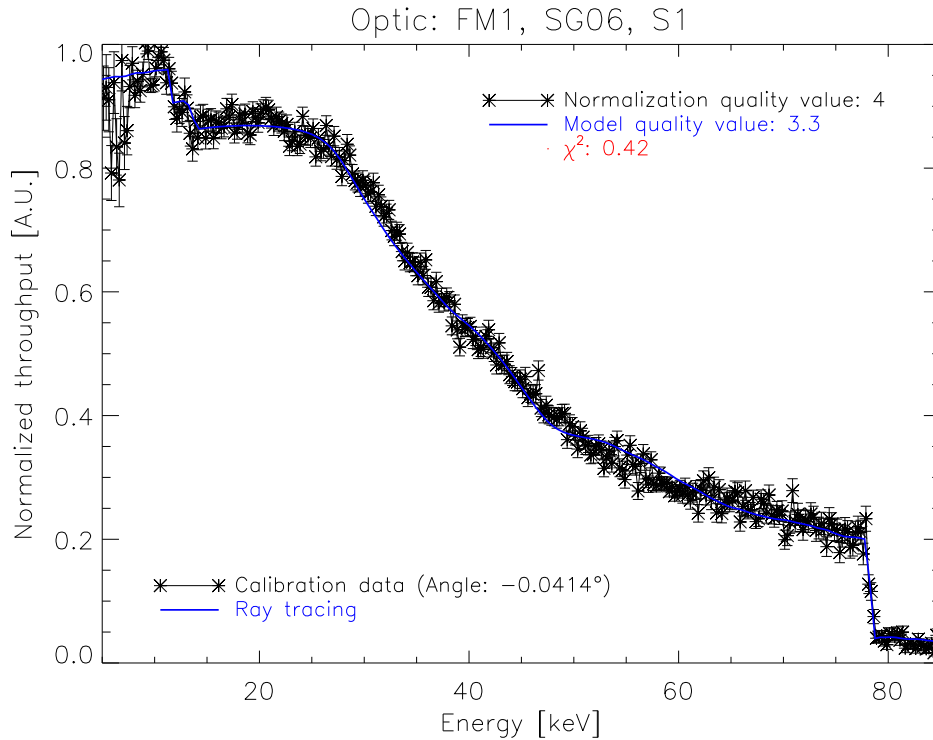
Figure 7. `ORM` prediction of reflectivity for a double reflection subgroup measurement.

6. MODEL QUALITY VALUE

For a number of witness samples, and the mounted substrates affiliated with them, weaknesses in the model are tracked and awarded points to describe the *potential* impact on the `ORM` estimates. The weaknesses may f.ex. be missing witness sample data or poorly determined d_{max}. The latter is caused by poor statistics at low energy. The awarded points are summed and divided by the total number of substrates under investigation, to give the Model Quality Value (`MQV`). An `MQV` of zero means that no known weaknesses exist for the data set. The maximum possible `MQV` is two-hundred, while the highest one recorded so far is seventy, with the vast majority below ten. At this stage the `MQV` has not been fully realized, but the intention is for it to assist in tracking down cause and solution to potential `ORM` deviations from data. An example of this is shown in Figure 8, where a non-zero `MQV` has been achieved due to a poorly determined d_{max} on a number of contributing substrates. Knowledge of said weakness allows the as-coated multilayer to be refit for the afflicted substrates using the on-ground calibration data.
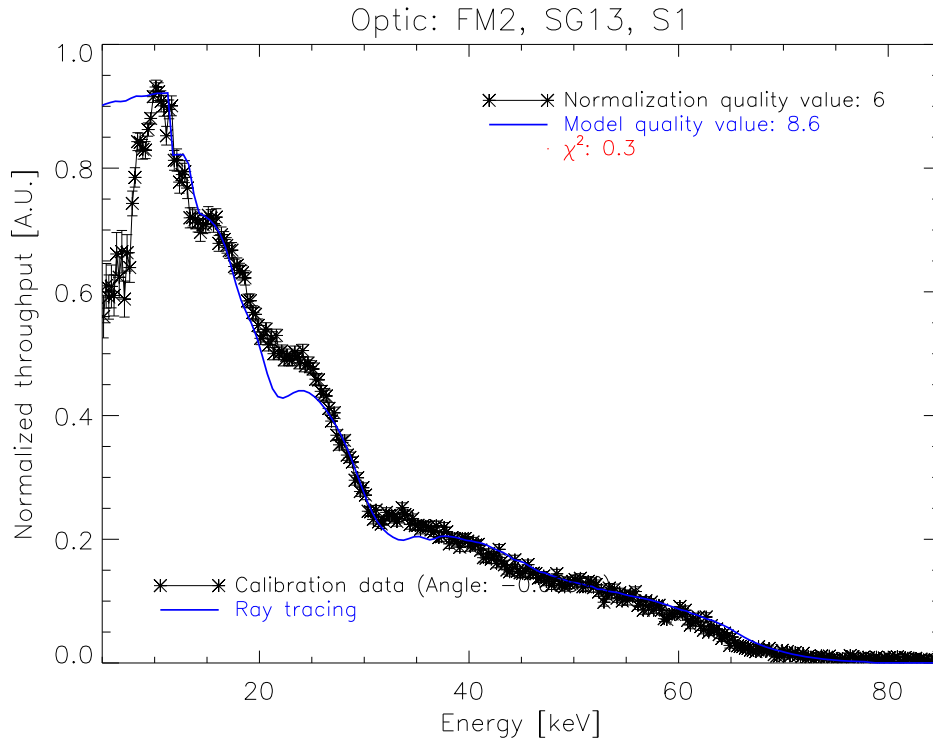
Figure 8. `ORM` prediction of reflectivity with a non-zero `MQV` caused by a poorly fit d_{max} value.

7. IN-ORBIT CALIBRATION

At the time of writing the in-orbit calibration of `NuSTAR` is ongoing and no data is available as yet. Instead the current best `ORM` predictions for the in-orbit A_{eff} of each of the two flight optics are given in Figure 9 and Figure 10. For comparison the effective area assuming the intended multilayer recipes summarized in Table 1 has also been plotted, including the actual figure error and non-specular reflectivity. The estimated A_{eff} including the `MRD` is lower as a result of the combined influence of the 15% higher micro-roughness on slumped glass compared to `Si` wafers, coating non-uniformities and the reduced bilayer thickness values established through the extensive witness and uniformity campaigns.
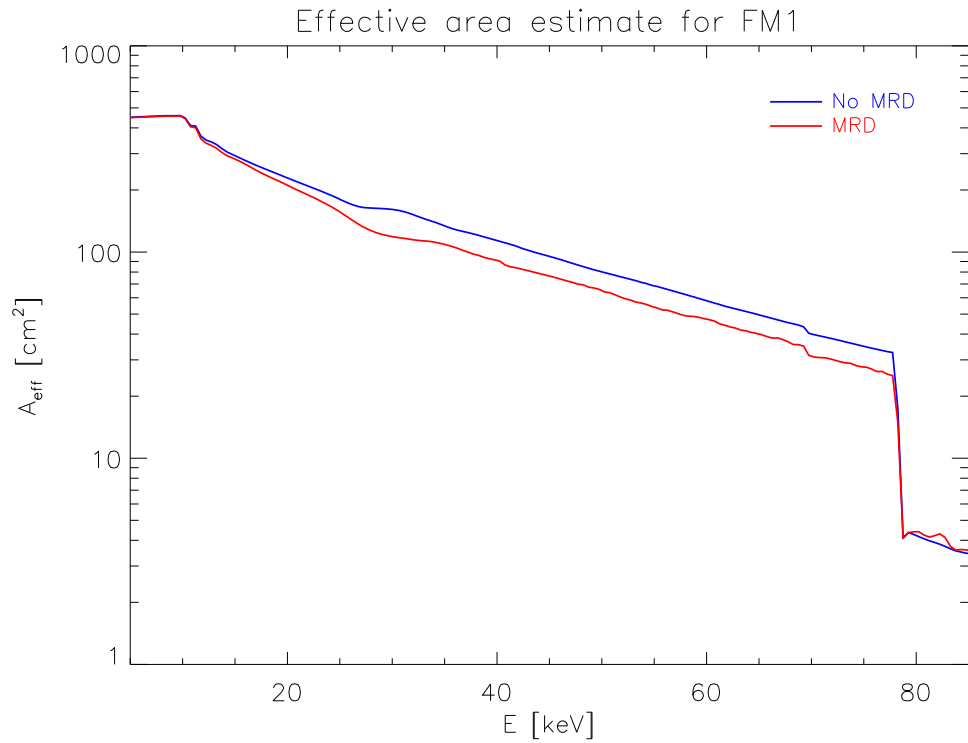
Figure 9. ORM prediction of the in-orbit on-axis A_{eff} for Flight Module 1 (FM1), with and without the use of the MRD.
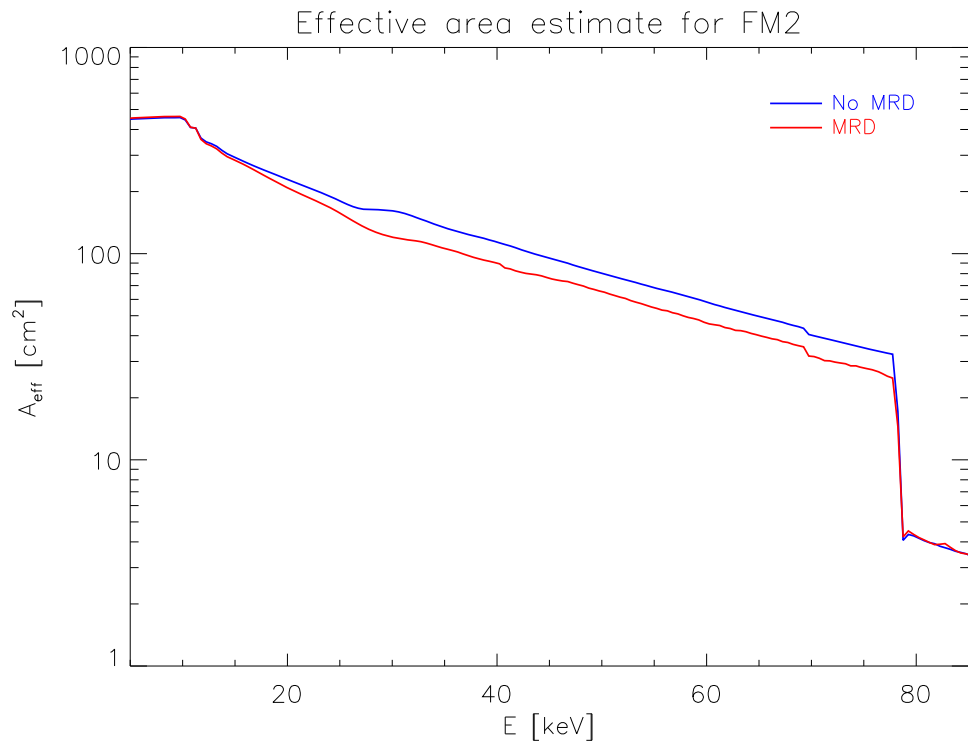

Figure 10. ORM prediction of the in-orbit on-axis A_{eff} for Flight Module 2 (FM2), with and without the use of the MRD.

ACKNOWLEDGMENTS

References

[1] F. A. Harrison, S. Boggs, F. E. Christensen, W. Craig, C. Hailey, D. Stern, W. Zhang, L. Angelini, H. An, V. Bhalereo, N. F. Brejnholt, L. Cominsky, W. R. Cook, M. Doll, P. Giommi, B. Grefenstette, A. Hornstrup, V. Kaspi, Y. Kim, T. Kitaguchi, J. Koglin, C. C. Liebe, G. Madejski, K. Kruse Madsen, P. Mao, D. Meier, H. Miyasaka, K. Mori, M. Perri, M. Pivovaroff, S. Puccetti, V. Rana, and A. Zoglauer, "The Nuclear Spectroscopic Telescope Array (NuSTAR)," in *Space Telescopes and Instrumentation 2010: Ultraviolet to Gamma Ray*, vol. 7732, no. 1, 2010, pp. 77 320S–8.

[2] N. F. Brejnholt, F. Christensen, C. Hailey, J. Koglin, K. L. Blaedel, H. An, B. Grefenstette, K. K. Madsen, J. K. Vogel, N. Barriere, J. Brown, T. A. Decker, Z. Haider, A. C. Jakobsen, C. P. Cooper-Jensen, M. J. Pivovaroff, C. Sleator, S. D., M. Stern, W. W. Craig, K. Mori, G. Tajiri, D. Thornhill, J. Cushman, and M. Nynka, "The Rainwater Memorial Calibration Facility (RaMCaF) for X-ray optics," *X-ray Optics and Instrumentation*, vol. 2011, p. Online, 2011.

[3] N. F. Brejnholt, F. Christensen, C. Hailey, J. Koglin, K. L. Blaedel, K. K. Madsen, J. K. Vogel, T. A. Decker, A. C. Jakobsen, M. J. Pivovaroff, C. Sleator, M. Stern, W. W. Craig, and D. Thornhill, "NuSTAR ground calibration: The Rainwater Memorial Calibration Facility (RaMCaF)," in *Optics for EUV, X-Ray, and Gamma-Ray Astronomy*, vol. 8147, no. 16, 2011.

[4] F. E. Christensen, N. F. Brejnholt, and A. J. Jakobsen, "Coatings for the NuSTAR mission," in *Astronomical Optics and Instrumentation*, vol. 8147, no. 29, 2011.

[5] J. E. Koglin, H. An, K. L. Blaedel, N. F. Brejnholt, F. E. Christensen, W. W. Craig, T. A. Decker, C. J. Hailey, L. C. Hale, F. A. Harrison, C. P. Jensen, K. K. Madsen, K. Mori, M. J. Pivovaroff, G. Tajiri, and W. W. Zhang, "NuSTAR hard x-ray optics design and performance," in *Optics for EUV, X-Ray, and Gamma-Ray Astronomy*, vol. 7437, no. 1, 2009, pp. 74 370C–8.

[6] N. J. S. Westergaard, K. K. Madsen, J. E. Koglin, N. F. Brejnholt, F. E. Christensen, M. J. Pivovaroff, and J. K. Vogel, "NuSTAR on-ground calibration: Imaging quality," in *Proceedings of SPIE*, 2012.

[7] N. F. Brejnholt, "NuSTAR calibration facility and multilayer reference database," *ORBIT*, vol. ISBN 978-87-92477-11-8, p. Ph.D. thesis, December 2011.

[8] N. J. S. Westergaard, "MT_RAYOR: a versatile ray tracing tool for X-ray telescopes," in *Proceedings of SPIE*, vol. 8147, 2011.

[9] J. E. Koglin, H. An, K. L. Blaedel, N. F. Brejnholt, F. E. Christensen, W. W. Craig, T. A. Decker, C. J. Hailey, L. C. Hale, F. A. Harrison, C. P. Jensen, K. K. Madsen, K. Mori, M. J. Pivovaroff, G. Tajiri, and W. W. Zhang, "First results from the ground calibration of the NuSTAR flight optics," in *Optics for EUV, X-Ray, and Gamma-Ray Astronomy*, vol. 8147, no. 17, 2011, pp. 74 370C–8.